

Retrieval of Individualized Head-Related Transfer Functions for Hearing Aid Applications

Michael Buerger, Stefan Meier,
Christian Hofmann, Walter Kellermann
Multimedia Communications and Signal Processing
Friedrich-Alexander University Erlangen-Nürnberg
91058 Erlangen, Germany
Email: {Buerger, SMeier, Hofmann, WK}@LNT.de

Eghart Fischer, Henning Puder
Sivantos GmbH
91058 Erlangen, Germany
Email: {Eghart.Fischer, Henning.Puder}@sivantos.com

Abstract—The capability of modern hearing aids to provide hearing-impaired humans with enhanced signals, which ultimately leads to an increased speech intelligibility, may benefit from fitting the device for each subject individually. This ideally also involves the exploitation of Head-Related Impulse Responses (HRIRs). However, HRIRs vary from person to person and thus require tedious measurements for each individual. In this work, we investigate two approaches which aim at speeding up the HRIR acquisition procedure. These are continuous measurements and interpolation, where Dynamic Time Warping (DTW) as well as linear interpolation of the magnitude and phase responses are considered. In contrast to related publications, the continuous HRIR measurements are not performed in anechoic environments here. The quality of the obtained HRIRs is assessed by means of the system mismatch and the proposed error of relative transfer functions. Both measures reveal that continuous HRIR measurements are on average much more capable than the investigated interpolation approaches, and they furthermore provide a more uniform performance for different source directions.

I. INTRODUCTION

According to the World Health Organization (WHO), around 360 million people worldwide are currently suffering from hearing loss [1]. In order to help these people to at least partly recover their hearing capabilities, technical devices such as cochlea implants or, more commonly, hearing aids are utilized. Modern hearing aids accommodate multiple microphones per device, which allows for multichannel signal enhancement [2], and with the transmission of microphone signals between the left and right hearing aid comes the possibility to apply binaural approaches such as binaural beamforming. The purpose of these techniques is to provide spatial selectivity and to extract a desired sound source. The best performance may generally be achieved by taking into account how the pinnae, the head, and the torso affect the sound waves arriving at the ears. In particular, Interaural Time Differences (ITDs) and Interaural Level Differences (ILDs) resulting from head shadowing should be considered. These effects can be described in the frequency-domain with the help of Head-Related Transfer Functions (HRTFs), which characterize the propagation paths from a source to the ears. The corresponding time-domain representations are referred to as Head-Related Impulse Responses (HRIRs).

Due to the different sizes and shapes of the human pinnae, head, and torso, a particular set of HRIRs is only valid for a particular person. Accordingly, signal enhancement methods relying on the exploitation of HRIRs should be adapted to each person

individually. In the ideal case, this is achieved by an individual measurement of HRIRs for each hearing-impaired person and a setup with sound sources located at all practically relevant positions around the head. This obviously requires a lot of effort and is a very time-consuming process. One approach to mitigate this problem is to limit the HRIR measurements to few source directions only and to apply interpolation techniques [3]–[6] in order to obtain HRIR estimates for all remaining angles. The idea of continuous HRIR measurements, where the subject is rotating during the acquisition process, is an alternative approach and was previously investigated under anechoic conditions [7]–[9]. Publications dedicated to continuous measurements in reverberant environments, such as [10], are concerned with mere room impulse responses rather than HRIRs. In this contribution, the interpolation and continuous measurement of HRIRs is investigated for reverberant environments and in the context of hearing-aid applications.

The remainder of this paper is structured as follows: First, the procedure for measuring HRIRs is discussed in Sec. II, where both the general approach for fixed measurement positions as well as continuous measurements with a rotating subject are outlined. In Sec. III, two different interpolation methods—including one based on Dynamic Time Warping (DTW) [11]—are explained. The experimental results are presented in Sec. IV, before the work is concluded in Sec. V.

II. MEASURING HEAD-RELATED IMPULSE RESPONSES

Before the continuous measurement of Head-Related Impulse Responses (HRIRs) for a rotating subject is discussed in Sec. II-B, the general approach utilized in this work for measuring HRIRs is briefly outlined in Sec. II-A.

A. General Procedure

In order to measure HRIRs, perfect sequences [12]–[14], perfect sweeps [15], or Maximum Length Sequences (MLSs) [16] are commonly utilized. In this work, the HRIRs are obtained using MLSs $x[k]$ with a length of N samples, whose normalized cyclic auto-correlation function $R_{xx}[\kappa]$ is

$$R_{xx}[\kappa] = \frac{1}{N} \sum_{k=0}^{N-1} x[k] \cdot x[k + \kappa \bmod N] \quad (1)$$

$$= \begin{cases} 1 & \text{if } \kappa \bmod N = 0 \\ -\frac{1}{N} & \text{else} \end{cases} \quad (2)$$

The length of an MLS is given by $N = 2^n - 1$, where n denotes the order. For sufficiently high orders n (implying a long

sequence), R_{xx} corresponds to a unit impulse train featuring a single unit impulse in each period of length N . As the microphone signal $y[k]$ is given by the linear convolution of the MLS $x[k]$ and the impulse response $h[k]$, the cyclic auto-correlation function between $x[k]$ and $y[k]$ results in

$$R_{xy}[\kappa] \approx \sum_{\rho=-\infty}^{\infty} h[\kappa - \rho N] \quad (3)$$

for sufficiently large N . Consequently, each length- N period of R_{xy} starting at integer multiples of N provides a good estimate for $h[k]$ given that N is larger than the length N_h of $h[k]$. If the MLS is too short and $N < N_h$, the periodic repetitions of $h[k]$ do overlap and the tail of $h[k]$ occurs as “ghost peaks” due to cyclic convolution effects, which we refer to as temporal aliasing. Note that at least two periods of the MLS must be recorded in order to be able to observe a cyclic convolution in the microphone signal and to compute (3) accordingly, where the first N samples of the recording are discarded as they represent a linear convolution. The number of reproduced MLS periods, referred to as frames, may be increased further in order to reduce the impact of measurement noise by averaging multiple periods of R_{xy} .

As an alternative to computing the cyclic correlation R_{xy} , which is known as Inverse Cyclic Convolution (ICC), the Normalized Least Mean Squares (NLMS) algorithm can be applied to identify the HRIR from a given microphone signal. However, it was shown that the NLMS with a stepsize of one is equivalent to ICC when perfect sequences are used as excitation signals [17].

B. Continuous HRIR Measurements

Rather than measuring the HRIRs of a subject for a multitude of different directions, the subject can also be rotated during the measurement while continuously playing out MLSs and recording the according microphone signals. This approach has several implications: First of all, the estimate obtained from a recorded MLS frame now represents an “average” HRIR for a certain angular range and does not correspond to a single direction anymore. Consequently, the estimated HRIRs will not be equal to the HRIRs resulting from fixed measurements. For the same reason, averaging of multiple estimates resulting from different frames of the continuous measurements is generally not reasonable anymore, such that the susceptibility to noise of the resulting estimate is increased.

Achieving a good system identification performance and a fine angular resolution, where the rotation of the subject only covers a small angular range during the recording of an entire MLS frame, either requires a low rotation speed or a short length N of the MLS. However, with decreasing values of N , temporal aliasing may occur or its impact may become stronger, which can be avoided by decreasing the rotation speed and, thus, increasing the overall measurement duration.

To estimate HRIRs for different directions from a recording obtained with a continuously rotating subject, the microphone signal is first partitioned into possibly overlapping blocks of length $2N$ starting at sample N_0 . For each block, we can then compute the ICC which yields an HRIR estimate for a particular angular region. It should be noted that computing the ICC using non-disjoint blocks with $N_0 \bmod N = N_\Delta \neq 0$ would result in an HRIR estimate cyclically shifted by N_Δ samples. This can be compensated by also applying a cyclic shift of N_Δ samples to the MLS used for the ICC. As mentioned above, the individual HRIR estimates of the different frames are not averaged here in order to obtain the best possible angular resolution.

III. INTERPOLATION OF HEAD-RELATED TRANSFER FUNCTIONS

Another approach to efficiently acquiring HRIRs is to subsample the angular range, i. e., to measure HRIRs for few directions only and to interpolate the HRIRs for missing intermediate angles ϕ_{int} afterwards. For this purpose, Dynamic Time Warping (DTW) as well as a linear interpolation of the magnitude and phase responses of the HRTFs are considered here.

A. Dynamic Time Warping (DTW)

The concept of Dynamic Time Warping (DTW) was originally introduced in [11] in the context of automatic speech recognition. Its purpose is to nonlinearly warp two sequences of different lengths such that they are temporally aligned in the best way. Similar to [18], where DTW was used to align HRIRs, we apply the DTW-based alignment in the context of hearing aids here. A detailed description of the algorithm can be found, e. g., in [11] or [19]. Here, we only provide a very brief outline of the main steps. The alignment between two HRIRs $h_i[k]$ and $h_j[k]$ corresponding to directions ϕ_i and ϕ_j , respectively, is done by first computing the L_1 distances between all samples of each HRIR according to

$$\Delta h_{ij}[k_i, k_j] = |h_i[k_i] - h_j[k_j]|, \quad (4)$$

where $|\cdot|$ returns the absolute value. These distances represent costs, and the objective is to find the path

$$P[n] = [k_i[n], k_j[n]] \quad (5)$$

which results in the lowest accumulated cost obtained when walking through $\Delta h_{ij}[P[n]]$ along the path. Different approaches to finding this path are discussed in [19]. The warping/alignment process itself can be described as

$$h_{w,i}[n] = h_i[k_i[n]], \quad (6)$$

$$h_{w,j}[n] = h_j[k_j[n]]. \quad (7)$$

Once the alignment is done, the warped HRIRs can be linearly interpolated to obtain an estimate for an intermediate direction $\phi_{\text{int}} \in [\phi_i, \phi_j]$ according to

$$h_{w,\text{int}}[n] = \alpha h_{w,i}[n] + (1 - \alpha) h_{w,j}[n], \quad (8)$$

where α determines the relative weight of the individual HRIRs. It is defined as

$$\alpha = \frac{\phi_j - \phi_{\text{int}}}{\Delta\phi}, \quad (9)$$

with $\Delta\phi = \phi_j - \phi_i$ being the angular difference between the sampled directions. In the same way as $h_{w,i}$ and $h_{w,j}$, the corresponding original discrete-time indices k_i and k_j are interpolated,

$$k_{\text{int}}[n] = \alpha k_i[n] + (1 - \alpha) k_j[n]. \quad (10)$$

This allows for an unwarping of the interpolated HRIR, which may be expressed as

$$h_{\text{int}}[k_{\text{int}}[n]] = h_{w,\text{int}}[n]. \quad (11)$$

As the interpolated indices $k_{\text{int}}[n]$ are generally not equidistant and do not coincide with the original discrete-time axis k , both the time axis $k_{\text{int}}[n]$ and $h_{w,\text{int}}[k_{\text{int}}[n]]$ are interpolated, e. g., using splines, in order to obtain the corresponding values at k . This last step yields the final result of the interpolated impulse response $h_{\text{int}}[k]$.

B. Linear Interpolation of Magnitude and Phase

An interpolation of HRIRs is generally only reasonable after a temporal alignment of peaks which are caused by the same wave front, but occur at different locations of the respective HRIR. Nevertheless, the magnitudes $A(\omega)$ and phases $\varphi(\omega)$ of the corresponding HRTFs $H(\omega)$ may be interpolated. The HRTF obtained from interpolating the magnitude and phase responses of two HRTFs $H_i(\omega) = A_i e^{j\varphi_i(\omega)}$ and $H_j(\omega) = A_j e^{j\varphi_j(\omega)}$ for directions ϕ_i and ϕ_j , respectively, and a target direction ϕ_{int} is given by [5]

$$H_{\text{int}}(\omega) = A_{\text{int}}(\omega) e^{j\varphi_{\text{int}}(\omega)}, \quad (12)$$

with the interpolated magnitude

$$A_{\text{int}}(\omega) = \alpha A_i(\omega) + (1 - \alpha) A_j(\omega), \quad (13)$$

the interpolated phase

$$\varphi_{\text{int}}(\omega) = \alpha \varphi_i(\omega) + (1 - \alpha) \varphi_j(\omega), \quad (14)$$

and α as defined in (9). It is important to stress that an unwrapping of the phase responses is required prior to interpolation, as all computations are performed for discrete frequency bins in the Discrete Fourier Transform (DFT) domain, where the unwrapping process constitutes a potential source of errors.

IV. EXPERIMENTS

In this section, we first discuss the setup underlying the experiments and introduce the considered performance measures in Sec. IV-A, before the HRIRs obtained with continuous measurements and interpolation are assessed in Sec. IV-B and Sec. IV-C, respectively. A brief performance comparison is given in Sec. IV-D.

A. Experimental Setup and Evaluation Measures

For the experiments, a KEMAR [20] mannequin was mounted onto a motorized rotor such that its orientation could be adjusted precisely. KEMAR was equipped with behind-the-ear hearing aid housings, each of which accommodates two microphones with a spacing of about 1 cm. The distance between the loudspeaker diaphragm and the center of the hearing aids was approx. 90 cm, as illustrated in Fig. 1. KEMAR's look direction ϕ is specified w. r. t. the fixed loudspeaker position, where $\phi = 0^\circ$ corresponds to the frontal direction and the angular range $0^\circ < \phi < 180^\circ$ corresponds to the loudspeaker being located on the right-hand side. All HRIRs were recorded at a sampling frequency of 48 kHz in an acoustic lab with reverberation time $T_{60} \approx 120$ ms. For evaluation, however, only the direct paths of the HRIRs were considered, i. e., the HRIRs were truncated accordingly, as room-specific reflections should not be taken into account when designing HRIR-based signal enhancement algorithms such as beamforming. Nevertheless, reverberation was present during the recordings. The ground truth was measured in five-degree steps for fixed directions $\phi \in \{-90^\circ, -85^\circ, \dots, 90^\circ\}$, with a measurement duration of 5 s for each angle, and a periodically repeated MLS with frames of length $L = 340$ ms ($N = 16383$ samples).

To assess the quality of the estimated HRIRs obtained from the continuous measurements or via interpolation, the following two performance measures are evaluated. As a first measure, the system mismatch [21] is utilized, which describes how well the estimated HRIRs match the true ones. It is defined as

$$D_m(\phi) = \frac{\|\mathbf{h}_m(\phi) - \hat{\mathbf{h}}_m(\phi)\|_2}{\|\mathbf{h}_m(\phi)\|_2}, \quad (15)$$

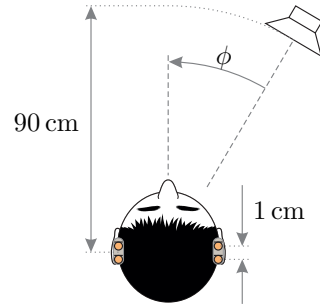


Fig. 1. Evaluation setup

where $\|\cdot\|_2$ denotes the L_2 norm, $\mathbf{h}_m(\phi)$ and $\hat{\mathbf{h}}_m(\phi)$ are column vectors capturing the samples of the true HRIR $h_m[k, \phi]$ and the estimated HRIR $\hat{h}_m[k, \phi]$, respectively, for a certain direction ϕ , and $m \in \{\text{left front, left rear, right front, right rear}\}$ indicates the microphone channel.

As for multichannel speech enhancement algorithms such as beamforming, mainly the Relative Transfer Functions (RTFs) between the individual microphone channels are of interest, we also introduce the normalized error of relative transfer functions. This frequency-dependent measure is defined as

$$e_{\text{RTF},m}(\omega, \phi) = \frac{\left| \frac{H_m(\omega, \phi)}{H_{\text{ref}}(\omega, \phi)} - \frac{\hat{H}_m(\omega, \phi)}{\hat{H}_{\text{ref}}(\omega, \phi)} \right|}{\left| \frac{H_m(\omega, \phi)}{H_{\text{ref}}(\omega, \phi)} \right|}, \quad (16)$$

where $H_{(\cdot)}$ and $\hat{H}_{(\cdot)}$ denote the true and estimated HRTFs, respectively, and the RTFs are computed w. r. t. the reference microphone channel indicated by the subscript $(\cdot)_{\text{ref}}$.

It should be noted that only frequencies below 8 kHz are evaluated here, as this frequency range can be considered most important in hearing aid scenarios.

B. Continuous HRIR Measurements

The continuous measurements were carried out choosing three different, but constant rotation speeds, and a rotation of KEMAR from $\phi = +90^\circ$ to $\phi = -90^\circ$ took 4 s, 8 s, and 16 s, respectively. The loudspeakers were playing out periodically repeated MLSs, where frames of length $L = 85$ ms ($N = 4095$ samples), $L = 170$ ms ($N = 8191$ samples), and $L = 340$ ms ($N = 16383$ samples) were considered. The sound level at the ear positions was approx. 55 dB(A). To match the ground truth data with the HRIR estimates $\hat{h}_m[k, \phi]$ obtained from the continuous recordings using ICC, a correlation-based Direction Of Arrival (DOA) estimation was utilized. That is, the DOAs were first estimated for all HRIRs $h[k, \phi]$ and for all estimates $\hat{h}_m[k, \phi]$. For each direction ϕ available in the ground truth data, the corresponding set of HRIR estimates with the most similar DOA was then assigned, such that no tracking of the orientation of KEMAR was required.

The system mismatch D_m resulting from the HRIR estimates thus obtained is shown in Fig. 2(a) for an MLS with a frame length of 170 ms and a rotation duration $T = 16$ s, where the values of D_m are truncated at -30 dB. It can be seen that the system mismatch for the two microphones in the same hearing aid is very similar. Furthermore, a performance degradation is present for the microphones in the left hearing aid in case the sound source is located to the right front, i. e., in the angular region between $20^\circ < \phi < 45^\circ$. Apart from that, no clear pattern can be observed except for a very slight tendency towards lower values of D_m for $\phi > 0$. The performance is, however, generally decent for all directions.

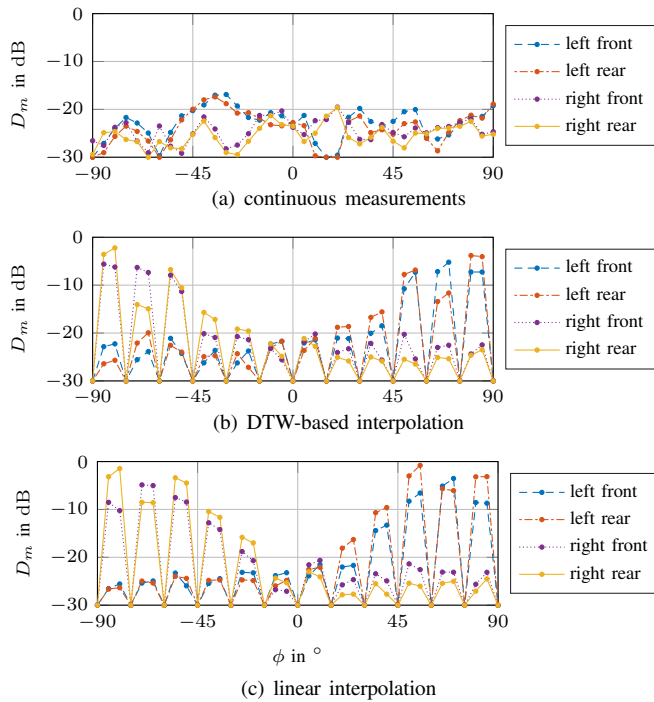


Fig. 2. System mismatch D_m resulting from HRIR interpolation with $\Delta\phi = 15^\circ$ and continuously measured HRIRs with $T = 16$ s and $L = 170$ ms.

The averaged values of the system mismatch for all directions ϕ and microphone channels m are listed in Table I(a) for the different tested rotation durations and frame lengths. As expected, the longer the rotation duration T is, i. e., the lower the rotation speed is, the better the system identification performance will be. Interestingly, an increase in the frame length L of the MLS results in larger values of the system mismatch for $T = 4$ s and $T = 8$ s, whereas the system mismatch is reduced even further for $T = 16$ s. This shows that the angular resolution provided by the longest rotation duration is not the limiting factor for the system identification performance, but the HRIR estimates are more impaired by other effects such as background noise and/or reverberation. In contrast, the limited angular resolution resulting from shorter rotation durations has a significantly larger impact on the performance than reverberation and/or background noise.

The error $e_{\text{RTF},m}$ of the RTFs as resulting from the continuously measured HRIRs is illustrated in Fig. 3(a) for an MLS with a frame length $L = 170$ ms and a rotation duration $T = 16$ s. For the plots, the front right microphone is chosen as the reference channel, and the values are truncated at -40 dB for illustration purposes. As can be seen, the error of RTFs for the right rear microphone is very low for a sound source located at directions $\phi > 0^\circ$, i. e., in the right halfplane. In this case, the reference channel as well as the sound source are on the same side as the considered microphone channel, and the impact of head shadowing is thus very low. For sound sources in the left halfplane, the error values are larger, which is especially obvious for higher frequencies where head shadowing is more pronounced. Similarly, the error values for the left rear microphone are generally larger, where the reference channel is located at the opposite side of the head. Note that the plot for the left front microphone is not shown here as it is very similar to the one for the left back microphone and, thus, does not provide additional insights.

TABLE I
SYSTEM MISMATCH D_m IN dB AVERAGED ALONG ALL DIRECTIONS ϕ AND MICROPHONE CHANNELS m FOR HRIRs OBTAINED FROM CONTINUOUS MEASUREMENTS (A) AND INTERPOLATION (B).

(a) continuously measured HRIRs			
Length L of MLS frame	Duration T of rotation		
	4 s	8 s	16 s
85 ms	-21.7	-21.7	-22.6
170 ms	-18.0	-21.4	-23.1
340 ms	-11.0	-19.9	-24.2

(b) interpolated HRIRs					
Type of interpolation	Angular distance $\Delta\phi$ between samples				
	10°	15°	20°	30°	45°
DTW-based	-17.9	-14.3	-11.8	-9.1	-6.1
Linear	-15.1	-12.4	-11.7	-8.7	-6.2

C. Interpolation of HRIR Measurements

The evaluation of the DTW-based HRIR interpolation and the linear interpolation of the magnitude/phase responses of HRTFs was done for angular distances $\Delta\phi \in \{10^\circ, 15^\circ, 20^\circ, 30^\circ, 45^\circ\}$ between the samples. More precisely, it was assumed that HRIRs are available for directions $\phi_\nu = -90^\circ + \nu \cdot \Delta\phi$, with $\nu \in \{\mathbb{N}_0^+ \mid \nu \cdot \Delta\phi \leq 180^\circ\}$. The HRIRs for all intermediate directions were interpolated in steps of 5° .

The resulting system mismatch D_m is shown in Fig. 2(b) and Fig. 2(c) for $\Delta\phi = 15^\circ$, where the values in the plot are again truncated at -30 dB. It can clearly be seen that both the DTW-based and the linear interpolation approach perform well if the sound source is located in a frontal direction. For lateral sound sources, however, a good performance is only obtained for the ipsilateral hearing aid, i. e., if the sound source and the microphones are located at the same side of the head, whereas the system mismatch is very large for the contralateral hearing aid. Note that the low system mismatch for multiples of 15° is due to the fact that no interpolation is required as HRIRs are available for these angles.

Similarly to the above, the average system mismatch for all directions ϕ and microphone channels m is listed in Table I(b) for different sampling distances $\Delta\phi$ and both interpolation approaches. As expected, the system mismatch increases with increasing angular distance $\Delta\phi$ between the samples, i. e., the directions for which HRIRs are available. Except for $\Delta\phi = 45^\circ$, the DTW-based approach performs consistently better than a linear interpolation of the magnitude and phase responses, where the performance difference is most pronounced for low values of $\Delta\phi$.

The frequency-dependent error of RTFs is plotted in Fig. 3(b) and Fig. 3(c) for an angular difference $\Delta\phi = 15^\circ$ between the sampled directions. Again, only the two rear microphone channels are illustrated, the front right microphone is chosen as the reference channel, and the values of $e_{\text{RTF},m}$ are truncated at -40 dB for illustration purposes. Surprisingly, the error of RTFs for the right rear channel is clearly better in the frequency range below approx. 2 kHz when using linear interpolation. For the left rear channel, this only holds if the sound source is located in the front or right front. For all other directions and higher frequencies, the error values obtained with DTW and linear interpolation are rather comparable: There are certain frequency ranges and directions for which DTW performs better, whereas linear interpolation results in lower error values in other areas.

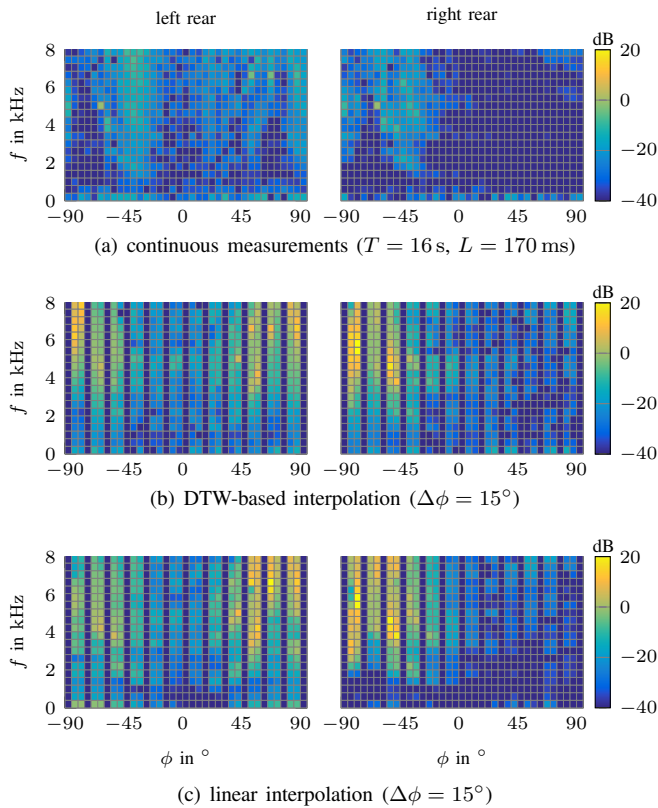


Fig. 3. Error of relative transfer functions $e_{\text{RTF},m}$ for the left rear and right rear microphones, where the right front microphone is the reference.

D. Discussion of Results

In terms of system mismatch, both interpolation approaches are clearly outperformed by continuous measurements with properly chosen parameters, as can be seen by comparison of Table I(a) and Table I(b). Moreover, a more uniform performance can be achieved with continuously measured HRIRs, whereas the system mismatch varies strongly for different angles when using interpolation (cf. Fig. 2). As far as the error of relative transfer functions is concerned, continuous HRIR measurements also clearly outperform both interpolation approaches (cf. Fig. 3). Only for very low frequencies and a few directions, linear interpolation achieves lower values of $e_{\text{RTF},m}$. However, the overall error of RTFs is still significantly larger in case of interpolation, even though the HRIRs are sampled at an angular spacing of $\Delta\phi = 15^\circ$, which can be considered rather dense already when counting the setup times for each individual direction of the HRIR measurement.

V. CONCLUSION

In this work, Head-Related Impulse Responses (HRIRs) for hearing aid devices are acquired from continuous measurements in reverberant environments and compared with HRIRs resulting from interpolation of fixed measurements. To assess the quality of the obtained HRIRs, the system mismatch and the proposed error of relative transfer functions are evaluated. The latter measure is independent of errors affecting all channels in the same way. It is thus especially relevant when it comes to spatial filtering techniques such as beamforming where time differences of arrival matter rather than actual angles. Both measures revealed that a continuous measurement of HRIRs is clearly superior to the investigated interpolation approaches, and it may thus be suited

as a practical procedure for acquiring individualized HRIRs to optimize multichannel speech enhancement algorithms in hearing aids. Assessing the resulting impact on the speech intelligibility in real-world scenarios remains a topic for future work.

ACKNOWLEDGMENT

The authors would like to thank Viktoria Heimann for her support in measuring numerous HRTFs.

REFERENCES

- [1] World Health Organization. (2015) Deafness and hearing loss. Accessed: 2017-01-28. [Online]. Available: <http://www.who.int/mediacentre/factsheets/fs300/en/>
- [2] S. Doclo, W. Kellermann, S. Makino, and S. E. Nordholm, "Multi-channel signal enhancement algorithms for assisted listening devices: Exploiting spatial diversity using multiple microphones," *IEEE Signal Process. Magazine*, vol. 32, no. 2, pp. 18–30, 2015.
- [3] K. Hartung, J. Braasch, and S. J. Sterbing, "Comparison of different methods for the interpolation of head-related transfer functions," in *Audio Eng. Soc. Conf.: 16th Int. Conf. on Spatial Sound Reproduction*. Audio Engineering Society, 1999.
- [4] F. P. Freeland, L. W. P. Biscainho, and P. S. R. Diniz, "Interpolation of Head-Related Transfer Functions (HRTFs): A multi-source approach," in *12th Europ. Sign. Proc. Conf. (EUSIPCO)*, Sept 2004, pp. 1761–1764.
- [5] S. Mehrotra, W.-G. Chen, and Z. Zhang, "Interpolation of combined head and room impulse response for audio spatialization," in *Proc. of Int. Workshop on Multimedia Signal Proc. (MMSp)*. IEEE, October 2011.
- [6] H. Gamper, "Head-related transfer function interpolation in azimuth, elevation, and distance," *J. Acoust. Soc. Am. (JASA)*, vol. 134, no. 6, pp. EL547–EL553, 2013.
- [7] T. Ajdler, L. Sbaiz, and M. Vetterli, "Dynamic measurement of room impulse responses using a moving microphone," *J. Acoust. Soc. Am.*, vol. 122, no. 3, pp. 1636–1645, 2007.
- [8] C. Antweiler and G.ENZNER, "Perfect sequence LMS for rapid acquisition of continuous-azimuth head related impulse responses," in *IEEE Workshop on Applicat. of Sign. Proc. to Audio and Acoust. (WASPAA)*, Oct 2009, pp. 281–284.
- [9] M. Rothbuecher, K. Veprek, P. Paukner, T. Habigt, and K. Diepold, "Comparison of head-related impulse response measurement approaches," *J. Acoust. Soc. Am. (JASA)*, vol. 134, no. 2, pp. EL223–EL229, 2013.
- [10] N. Hahn and S. Spors, "Comparison of continuous measurement techniques for spatial room impulse responses," in *24th Europ. Sign. Proc. Conf. (EUSIPCO)*, Aug 2016, pp. 1638–1642.
- [11] H. Sakoe and S. Chiba, "Dynamic programming algorithm optimization for spoken word recognition," *IEEE Trans. on Acoustics, Speech, and Signal Process. (ICASSP)*, vol. 26, no. 1, pp. 43–49, Feb 1978.
- [12] V. P. Ipatov, "Ternary sequences with ideal periodic autocorrelation properties," *Radio Eng. and Electron. Physics*, vol. 24, pp. 75–79, 1979.
- [13] H. D. Lüke, "Sequences and arrays with perfect periodic correlation," *IEEE Trans. on Aerospace and Electron. Syst.*, vol. 24, no. 3, pp. 287–294, 1988.
- [14] C. Antweiler and M. Antweiler, "System identification with perfect sequences based on the NLMS algorithm: Sequences and sets of sequences with low crosscorrelation and impulse-like autocorrelation and their applications," *AEU. Archiv für Elektronik und Übertragungstechnik*, vol. 49, no. 3, pp. 129–134, 1995.
- [15] A. Telle, C. Antweiler, and P. Vary, "Der perfekte Sweep—Ein neues Anregungssignal zur adaptiven Systemidentifikation zeitvarianter akustischer Systeme," *Jahrestagung für Akustik (DAGA)*, 2010.
- [16] J. Borish and J. B. Angell, "An efficient algorithm for measuring the impulse response using pseudorandom noise," *J. Audio Eng. Soc. (JAES)*, vol. 31, no. 7/8, pp. 478–488, 1983.
- [17] C. Antweiler, S. Kuehl, B. Sauer, and P. Vary, "System Identification with Perfect Sequence Excitation - Efficient NLMS vs. Inverse Cyclic Convolution," in *11. ITG Symp.: Speech Communication*, Sept 2014.
- [18] J. Bernhard, G. Gomez, and B. Seeber, "Time-domain interpolation of head-related transfer functions with correct reproduction of notch frequencies," *Jahrestagung für Akustik (DAGA)*, 2015.
- [19] M. Müller, *Information Retrieval for Music and Motion*. Springer, 2007.
- [20] M. D. Burkhard and R. M. Sachs, "Anthropometric manikin for acoustic research," *J. Acoust. Soc. Am. (JASA)*, vol. 58, no. 1, pp. 214–222, 1975.
- [21] P. Naylor and N. D. Gaubitch, *Speech Dereverberation*. Springer, 2010.